



circSnd1 promotes atherosclerosis progression through the miR-485-3p/Olr1 signaling pathway

Lin Yang^{*}, Yuhao Lin, Chao Wang, Pengcheng Fan

Vascular Surgery, The First Affiliated Hospital of Xi'an Jiaotong University, Xi'an, 710061, Shaanxi, China

ARTICLE INFO

Keywords:

Atherosclerosis
circRNA
ceRNA
circSnd1
miR-485-3p
Olr1

ABSTRACT

Background: Circular RNAs (circRNAs) participate in the development of atherosclerotic cardiovascular disease. Identifying and verifying the key competing endogenous RNA (ceRNA) network related to atherosclerosis (AS) is significant for understanding the development of AS. The aim of this study was to investigate the circRNA-miRNA-mRNA network, identify a key circRNA and explore its role in the development of atherosclerosis.

Methods: Differentially expressed mRNAs (DEMs) and circRNAs (DECs) in the AS model were obtained from datasets in the Gene Expression Omnibus (GEO) database. R software and Cytoscape software were used to construct and visualize the ceRNA network. The dual-luciferase reporter experiment and the RNA pull-down experiment were used to verify the selected ceRNA axis. siRNA targeting circRNA, miRNA mimic, miRNA inhibitor, or gene overexpression plasmid was used for *in vitro* functional studies. ELISA and western blotting were used to detect inflammation and lipid transport-related proteins. Furthermore, an AS mouse model was established and treated with recombinant adeno-associated viral vectors to further verify the influence of the selected ceRNA axis on the occurrence and/or development of AS.

Results: A total of 497 DEMs were enriched in 25 pathways, based on which the circ_0082139 (circSnd1)/miR-485-3p/Olr1 axis was selected. *In vitro*, the interaction among the three molecules of this axis was validated and it was found to affect inflammation and lipid transport, which were characterized by the significant change of inflammatory factors (Il-6, Il-8, Tnf- α , Mcp-1, Vcam-1, and Icam-1), and lipid transport-related genes, including Abca1, Abcg1, Ldlr, Hdlbp, Lp-pla2, and Srebp-1c. Through animal experiments, we further verified that the circSnd1/miR-485-3p/Olr1 axis regulated these molecules and participated in the formation and/or development of AS *in vivo*.

Conclusions: The circSnd1/miR-485-3p/Olr1 axis participates in the formation and development of atherosclerosis by regulating inflammation and lipid transport.

1. Introduction

Atherosclerosis (AS) is one of the leading causes of cardiovascular disease, which can lead to myocardial infarction and stroke [1,2]. AS is a cardiovascular disease caused by a variety of factors, including hypertension, diabetes, hyperlipidemia, and smoking. There are a series of key pathways involved in the development of atherosclerotic plaques, such as the cholesterol uptake pathway involving

^{*} Corresponding author.

E-mail address: jdvscs@126.com (L. Yang).

low-density lipoprotein receptor (LDLR) and the reverse cholesterol transport pathway involving ATP binding component protein A1 (ABCA1) [3]. Recently, it was found that a variety of circular RNAs (circRNAs) play important regulatory roles in the pathophysiological process of atherosclerosis, which can affect cell activity and proliferation, lipid metabolism, and inflammatory factor secretion [4–6]. For example, one study has shown that circ_RELL1 adsorbs miR-6873-3p in the cytoplasm, reduces NF- κ B activity and inflammatory factor levels, regulates inflammation, and provides anti-AS treatment with the circ_RELL1/miR-6873-3p/MyD88 axis [7]. However, the existing research on circRNAs is still in the preliminary stage. The follow-up development of circRNA in AS, patient prognosis, and clinical application remain issues that we need to explore continuously.

circRNAs participate in pathological and physiological processes through a variety of mechanisms, including the sponge effect of miRNA as a regulator of gene transcription and splicing, participating in the processing of ribosomal RNA, and acting as an aptamer for protein–protein interactions [8–11]. The sponge effect is the most researched topic at present. The construction and analysis of the competing endogenous RNA (ceRNA) network is a systematic method to discover the key circRNA in AS. Lipid metabolism is a key pathway for the formation and development of AS and is closely related to pathological changes such as inflammation, apoptosis, foam cell formation, and plaque instability. The phagosome pathway is a key pathway of the clearing function of macrophages, the formation of foam cells, and necrosis [12]. Macrophages phagocytose oxidized low-density lipoprotein (ox-LDL) through scavenger receptors, including CD36, Olr1 (also known as LOX-1), and CXCL-16, and then transform into macrophage-derived foam cells. At the same time, macrophages release inflammatory factors under pathological conditions, stimulate the cells to undergo apoptosis and necrosis, and then form AS plaques [13]. Therefore, focusing on the phagosome pathway, especially a ceRNA network analysis related to the scavenger hand, can identify key circRNAs in the occurrence and development of AS.

To discover the key circRNA in the development of atherosclerosis and verify its role, we constructed a ceRNA network related to key AS pathways using GEO data. After analyzing the key network, the macrophage AS model was constructed and used to verify the expression level of the selected molecules and related mechanisms. The dual-luciferase experiment and the RNA pull-down experiment were used to verify the accuracy of the ceRNA network. Furthermore, the mouse AS model and adeno-associated virus were used to further verify the role of the selected ceRNA network in AS *in vivo*.

2. Methods

2.1. Data acquisition

By searching the Gene Expression Omnibus (GEO) repository (<https://www.ncbi.nlm.nih.gov/gds>) with the keywords ox-LDL and atherosclerosis in human samples, two microarray datasets involving human THP-1 macrophages were obtained, namely, GSE107522 and GSE54666. In the GSE107522 dataset, we analyzed the circRNA expression profiles in three THP-1 macrophage samples with three foam cell samples as controls after stimulation with ox-LDL (50 mg/mL) for 24 h using an Agilent-069978 Arraystar Human CircRNA microarray, V1 (platforms: GPL19978). In the GSE54666 dataset, THP1 macrophages were treated with ox-LDL (50 mcg/mL) for 48 h to form foam cells or with control buffer, and each group had six independent biological replicates. The mRNA expression profiles were obtained using Illumina HumanHT-12, V4.0, Expression BeadChip (platforms: GPL10558).

2.2. Differential expression analysis and functional enrichment analysis

The GEO2R function embedded on the GEO website (<https://www.ncbi.nlm.nih.gov/gds>) was used to analyze the differential expression of circRNAs and mRNAs between the model and control groups, which were treated with or without ox-LDL. The differential circRNAs and mRNAs were annotated according to the corresponding platform information. A p value < 0.05 and $|\log_2FC$ (fold change) > 0.5 were defined as statistical threshold values to limit the target range. Kyoto Encyclopedia of Genes and Genomes (KEGG) pathway and gene ontology (GO) enrichment analyses were performed using DAVID Bioinformatics Resources v6.8 (<https://david.ncifcrf.gov/>).

2.3. circRNA-miRNA-mRNA ceRNA network construction

The interaction relationships among miRNAs, DEMs and DECs were predicted using the ENCORI database [14]. The one-to-one correspondence was constructed based on the ENCORI data using R software (version 3.5.3). The circRNA-miRNA-mRNA ceRNA network was visualized using Cytoscape software (version 3.8.2) [15]. The top ten core nodes in the ceRNA network were obtained through cytoHubba, a Cytoscape plugin.

2.4. Cell culture and treatment

Mouse RAW264.7 cells (catalog number: TCM13) were purchased from Cell Resource Center, Institute of Basic Medicine, Chinese Academy of Medical Sciences. RAW264.7 cells were cultured in Dulbecco's modified Eagle's medium supplemented with 10% FBS, 100 U/mL penicillin, and 100 μ g/mL streptomycin. The cells were treated in different ways according to the grouping needs. The normal group was routinely cultivated. The *in vitro* model of AS was prepared by stimulating mouse RAW264.7 cells with ox-LDL (50 μ g/ml) for 24 h. After the model was completed, operations such as plasmid transfection or virus infection were carried out. Following various treatments, the cells were collected for subsequent detection.

2.5. RNA isolation and real-time PCR

An RNA extraction kit (TAKARA, Dalian, China) was used to extract RNA from each group of tissues. Reverse transcription and quantitative PCR experiments were performed according to the instructions of the TAKARA reverse transcription and RT-PCR kit. The primers were mus-miR-485-3p, 5'-GCTCTAGTCATACACGGCTCTC-3' (F), 5'-GTGCAGGGTCCGAGGT-3' (R); mus_circSnd1, 5'-GAAACGGTGCCTGCCTTTTC-3' (F), 5'-CATACAGGGGCCGGAGCTTC-3' (R); mus-Olr1, 5'-GACAAGATGAAGCCTGCGAA-3' (F), 5'-AAGGGCCCATGGAAGAGGTA-3' (R); and mus-Gapdh, 5'-AATGGATTGGACGCATTGGT-3' (F), 5'-TTTGCCTGGTACGTGTTGAT-3' (R). The data were calculated using the $2^{-\Delta\Delta Ct}$ method and normalized to Gapdh (mRNA), U6 (miRNA) and 18S rRNA (circRNA).

2.6. Western blot analysis

Western blotting was used to detect the protein levels of Olr1, Hdlbp, Ldlr, Srebp-1c, Lp-pla2, Abcg1, Abca1, and Gapdh in RAW264.7 cells. Cells were routinely lysed to extract proteins. The extracted proteins were quantified using a BCA protein quantification kit (Thermo, USA). Conventional electrophoresis, membrane transfer, and antigen blocking operations were performed. Primary antibodies against Olr1 (dilution 1:1000; DF6522, Affinity, Melbourne, Australia), Hdlbp (1:1000; ab133594, Abcam, Cambridge, MA, USA), Ldlr (1:1000; DF7696, Affinity), Srebp-1c (1:1000; AF4728, Affinity), Lp-pla2 (1:1000; MA5-33112, Invitrogen, Carlsbad, CA, USA), Abcg1 (1:1000; ab52617, Abcam), Abca1 (1:1000; ab66217, Abcam), and Gapdh (1:5000; AB0037, Abways, Shanghai, China) were added to the incubation and incubated overnight in a box at 4 °C. The next day, the secondary antibody was added after the primary antibody was rinsed. Imaging agent (Tianneng, Shanghai, China) was added to the PVDF membrane to stain proteins. The experiments were repeated three times.

2.7. Enzyme-linked immunosorbent assay (ELISA)

ELISA kits were used to detect the expression levels of proinflammatory factors, including Il-6 (ab275971, Abcam), Il-8 (ab7747, Abcam), Tnf- α (ab183218, Abcam), Mcp-1 (ab9858, Abcam), Vcam-1 (ab223591, Abcam), and Icam-1 (ab174445, Abcam). The required plates were removed from the aluminum foil bag after equilibrating at room temperature for 20 min. Standards with different concentrations were added to the standard wells, and the standard curve was prepared by routine operation. Fifty microliters of the sample and horseradish peroxidase (HRP)-labeled detection antibodies were added to the sample well. The plates were sealed and shaken on a shaker for 3 h. After the routine washing operation, 100 μ L of substrate solution was added to each test well and incubated at room temperature for 15 min. The stop reaction solution (100 μ L) was added to stop the reaction. The OD value of each well was detected at 450 nm using a microplate reader.

2.8. Plasmid construction and transfection

The interference and overexpression plasmids for circSnd1, miR-485-3p, and Olr1 were designed by Sangon Biotech (Shanghai, China). The sequences of the siRNAs, shRNAs, miRNA mimics and miRNA inhibitors are listed in Supplementary Table S1. The cDNA of Olr1 was amplified by PCR using primers with HindIII/EcoRI restriction sites: 5'-CCC AAGCTT ATGACTTTTGATGACAAGATG-3' (forward), 5'-CCG GAATTC CTAAATTTGCAAATGATT TGTC-3' (reverse). According to the manufacturer's instructions, Lipofectamine 2000 (Invitrogen) was used to transfect siRNA or overexpression plasmid into 293T cells to amplify the plasmid and then purify the plasmid. The plasmid was transfected into RAW264.7 cells cultured in a six-well plate. After 6 h of transfection, the basal medium was refreshed, and culture continued for 48 h.

2.9. Luciferase reporter assay

The binding sequence of mus-miR-485-3p (miR-485-3p-wt) and mus-circSnd1 and mus-Olr1 mRNA wild-type 3'-untranslated region (3'-UTR) was obtained through NCBI. Mutant circSnd1 (circSnd1-mut) and mutant Olr1 (Olr1-mut) without the miR-485-3p binding site were obtained by overlapping extension PCR using mutant primers. For dual luciferase activity determination, the wild-type or mutant sequence of circSnd1 or Olr1 was cloned into the 3'-UTR of the Renilla luciferase gene in the pRL-TK plasmid. The above plasmids were cotransfected with the corresponding miRNA mimics or inhibitors into 293T cells. Firefly luciferase was used as a pGL3 control to monitor transfection efficiency. Luciferase detection was performed according to the instructions of the dual-luciferase reporter gene detection kit.

2.10. RNA pull-down

miR-485-3p and oligo were biotinylated to generate bio-miR-485-3p and bio-oligo probes by GenePharma Company (Shanghai, China). RAW264.7 cells were transfected with bio-miR-485-3p and bio-oligo probes for 48 h. The treated cells were lysed using lysis buffer and were incubated with Dynabeads M-280 Streptavidin (Invitrogen, cat. no. 11205D) by referring to the experimental instructions. Beads were incubated with biotinylated miR-485-3p for 10 min. After washing, the bound RNAs were examined by RT-qPCR assay.

2.11. AAV construction

An adeno-associated viral (AAV) vector delivery system was used for overexpression or silencing of the target genes. Briefly, a vector harboring mir-485-3p (AAV-mir-485-3p) or a short hairpin RNA targeting circSnd1 (AAV-sh-circSnd1) or Olr1 (AAV-sh-Olr1) was constructed by ligating the corresponding sequences containing the restriction enzyme cutting sites (HindIII/XhoI; Supplementary Table S1) into the transfer plasmid pAAV-AC-GFP and packaging into AAV-9 capsids using pAAV2/9n (packaging plasmid containing Rep/Cap genes) and pAdDeltaF6 (helper plasmid) in HEK293T cells. Through iodixanol gradient centrifugation, viral particles in the

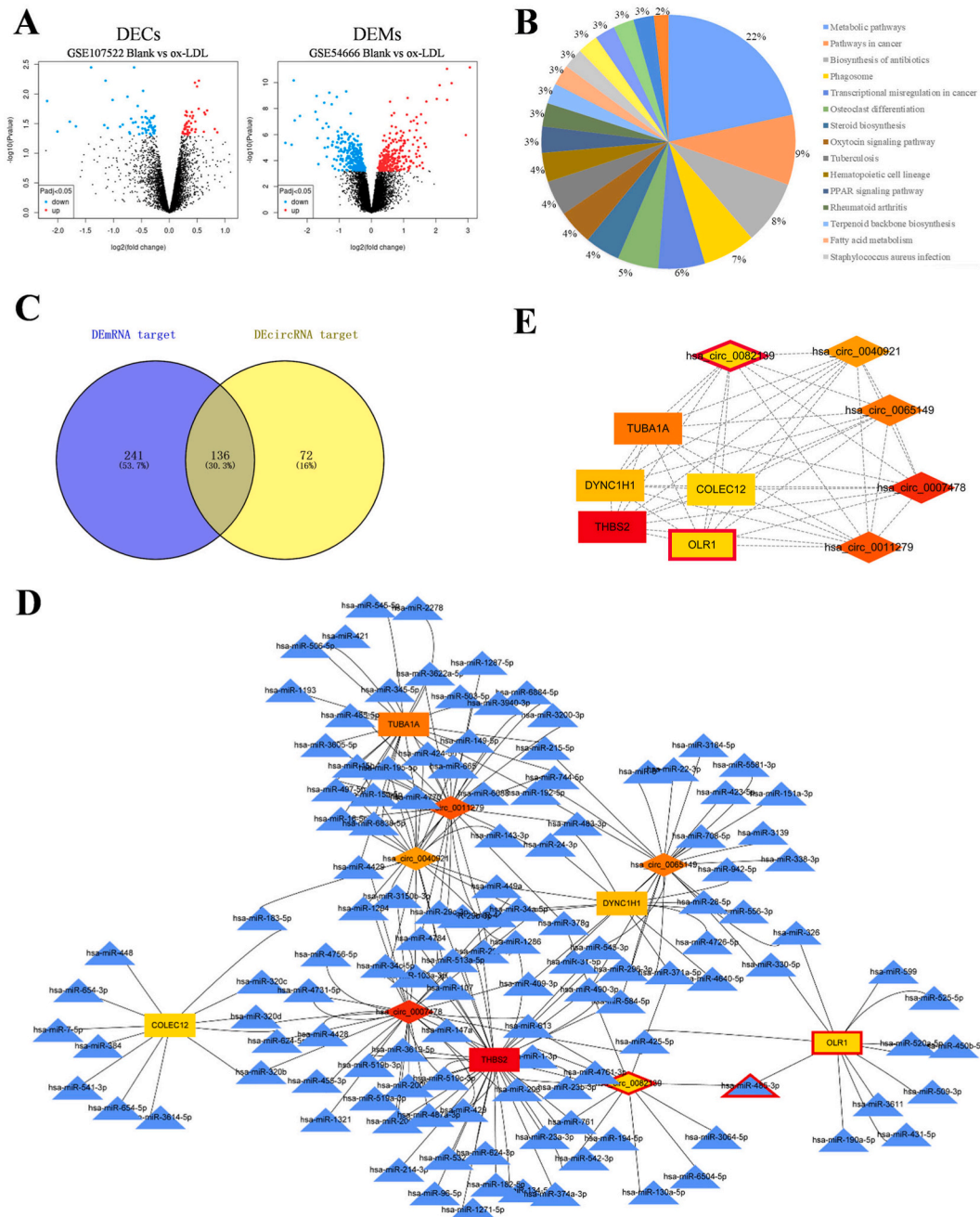


Fig. 1. AS-related circRNA-miRNA-mRNA ceRNA network construction and analysis. A, The differentially expressed mRNAs (DEMs) and circRNAs (DECs) in human macrophages after treatment with ox-LDL. B, KEGG pathway enrichment analysis of differentially expressed mRNAs. C, Predicted miRNAs that interact with the above DECs and DEMs in the phagosome pathway. D, ceRNA networks based on the overlapping miRNAs. E, Ten core nodes in the ceRNA network were further obtained by cytoHubba analysis. The selected hsa_circSnd1, hsa-miR-485-3p, and Olr1 (Olr1) are marked with a red frame.

Table 1
Differentially expressed circRNAs (DECs).

P value	t	log ₂ FC	SPOT_ID	circbase_ID	circAltas ID	Sequence
0.00356	4.60059	0.63157	hsa_circRNA_102030	hsa_circ_0007085	hsa-SUZ12_0028	ACTCAAACATATTGAGGCTGCCTCCATTGCAAAACATTTTCTCAGGGA
0.00357	4.59853	1.40261	hsa_circRNA_101031	hsa_circ_0007478	hsa-TM7SF3_0006	GTGCTTCCTAGACTCTCTTTCCAATTCCTCGGAAACAGGCACTG
0.00596	4.13149	1.14316	hsa_circRNA_101055	hsa_circ_0026218	hsa-CERS5_0011	ATCCATTCTGATTTATTGCCAAACCCCTGTGCACCTCTGTATTGGCAT
0.00597	-4.129597	-0.53229	hsa_circRNA_104442	hsa_circ_0006501	hsa-CUX1_0006	AGGAGGTGCTGACGGACAACAACCTGAAAGCACTCCAAGACCTC
0.01112	3.59907	0.75019	hsa_circRNA_102765	hsa_circ_0055201	hsa-SFXN5_0011	CTCCATTGCTACGTCCTTCTATGGCCGCTTCAGGCACCTTCTGGAT
0.0126	3.49655	1.01765	hsa_circRNA_400048	hsa_circ_0092327	-	TCTCACATCTCCCTGTGGCCTCTCCTTGGCATTAGAAAGCCAGGGA
0.01313	3.4627	2.19209	hsa_circRNA_100696	hsa_circ_0008896	hsa-PLPP4_0001	CATTCTCCTGCAATTTCTTCTCACACCCCTGGCTGTATTGT
0.01592	3.30826	0.56735	hsa_circRNA_100758	hsa_circ_0050486	hsa-GPI_0002	GAGCTGCCTCAAGAGCATTATGCCAGTACATACAGGCTTCTAAAGC
0.01774	-3.222224	-0.528753	hsa_circRNA_103342	hsa_circ_0065149	hsa-SETD2_0010	TATTCACAGACAACCTCCACCAATTGTACAGCACTGAACGAGGAAG
0.01895	-3.170605	-0.680023	hsa_circRNA_104468	hsa_circ_0082139	hsa-SND1_0014	ACCATTGGAGGAATGATAAGAACAAGAACTGCGTCCCTGTATGA
0.02051	-3.108706	-0.63005	hsa_circRNA_102411	hsa_circ_0048492	hsa-MFSD12_0001	CGGCACCTCAGGCACCGTCTGCGTCTGCTGTCTTCCCCTTCATCT
0.02203	-3.053476	-0.646782	hsa_circRNA_100139	hsa_circ_0011279	hsa-SERINC2_0001	CAAGGTCCAGGCGTCTGCTCTGCGGCTCTGCCCTGCATCTCTG
0.02606	2.92441	0.68563	hsa_circRNA_103685	hsa_circ_0070284	hsa-CDS1_0016	CCATTAATTAAGTTCGCATGGACTCATGTCACTTTACTGATAACTG
0.02932	2.83505	1.78564	hsa_circRNA_102513	hsa_circ_0050486	hsa-GPI_0002	TCCTCCCTGTTTCATCATTGGCTCCAAGCGTGTCCGGAGCGGTGACT
0.02983	2.82202	0.60567	hsa_circRNA_100453	hsa_circ_0008659	hsa-PTPN14_0004	ATCCTCTCTGACCAATCATGAAACTGTGTACACCTTGGCATTTC
0.03052	2.80486	0.65102	hsa_circRNA_100177	hsa_circ_0011692	hsa-STK40_0002	CCTCTTCCAGGTCCCGTCTGGGCACTCACCGGTGCCAAGCATAG
0.03284	2.74972	0.83615	hsa_circRNA_103352	hsa_circ_0001292	hsa-SCAP_0005	GGCTGAGTGGGTACCTGCACATGTTGTTCTTGTGCTGCTGTCAA
0.03345	2.73586	1.16595	hsa_circRNA_103329	hsa_circ_0064924	-	TTGGCCTCAGCTCTTGAGGATCTTGCTTGTCCAACCAGAGACA
0.03513	2.69926	1.67531	hsa_circRNA_101744	hsa_circ_0005699	hsa-C16orf62_0032	CTCTCCAAGGTGGGAATGGAAGTGGCCACATCTCAAAGAAACC
0.03559	2.68958	0.88334	hsa_circRNA_101223	hsa_circ_0029605	hsa-MPHOSPH8_0001	TTGAGCTTCTGTTTTTCTGGAATCCAGTGGAAATGACACTGGTGAT
0.03597	2.68163	0.55821	hsa_circRNA_102002	hsa_circ_0003645	hsa-C16orf62_0004	ATGACCCCTTTCATGGCCTCCAGATTACCAGACCAGAGCACTTGG
0.0375	2.65076	1.10481	hsa_circRNA_400071	hsa_circ_0092283	-	TCGCCAAGGTCCAGGACTTCTCCACTCTGGGCTCTGGCTGGAGCCA
0.03898	-2.622102	-0.817367	hsa_circRNA_101906	hsa_circ_0040921	-	ATGACAAGTATGACCGCATGAAGATCGCACCCCTCCCTCCCTGGC
0.04295	2.55034	2.00645	hsa_circRNA_101748	hsa_circ_0003645	hsa-C16orf62_0004	CTCTCCCAAGTGCACCTCACTTTGAGGATGAGAAAAGAATGCTGC
0.04332	-2.54403	-0.621634	hsa_circRNA_102462	hsa_circ_0049700	hsa-CC2D1A_0003	AGGCTCATCAAGTGGCGCTGCCCTGTCAACAAGGACGACTTTGC
0.04411	2.53078	0.71607	hsa_circRNA_400065	hsa_circ_0092317	-	TAGGAGAGAAGTGTGCCCACTCTCTGTGGGGGACCTGTACGCCAC
0.04435	-2.526696	-0.863075	hsa_circRNA_104317	hsa_circ_0079485	hsa-ISPDI_0027	GATTATTAAGGTGTAGTGACTATGACTTGGAAATTTGGAAGTGTG
0.04664	2.48986	0.70542	hsa_circRNA_101145	hsa_circ_0028198	hsa-RP11-478C19_0001	AAGACAAAGAAGTCCCAATGAGTTATTCTCCCACTCAGAAGTA
0.04756	2.47552	0.54069	hsa_circRNA_101078	hsa_circ_0026978	hsa-CS_0003	CCATCCACAGGGCATCCGTTTCCGAGGCTTATGATCCCTGAATGC

clarified supernatants were purified [16]. Gradient fractions containing virus were concentrated using Amicon UltraCel columns (Millipore) and stored at -80°C . C57BL/6 mice were injected with AAV particles using an insulin syringe with an incorporated 30-gauge needle.

2.12. Animals and treatments

Nine-week-old male C57BL/6 mice were purchased from Slack Laboratory Animal Co., Ltd. (Shanghai, China). Follow-up experiments were carried out after one week of adaptive feeding. All mice were kept at a constant temperature (22°C), humidity (relative humidity, 30%), and 12-h light-dark cycle with free access to food and water. The experimental operation process followed the Laboratory Animal Guideline for Ethical Review of Animal Welfare (GB/T 35892-2018) and was approved and supervised by the Animal Protection and Use Agency Committee of The First Affiliated Hospital of Xi'an Jiaotong University (approval number: 2019LSK-G-6). Mice were fed normal chow or an atherogenic diet containing 1.25% cholesterol, 15% fat, and 0.5% cholic acid [17]. The animals were euthanized using intraperitoneal injection with 60 mg/kg body weight sodium pentobarbital. Hematoxylin-eosin (HE) staining was used for model identification. Two hundred microliters of injection containing 1×10^{11} VG/mL AAV virus was injected through the tail vein. After 16 weeks of rearing, the thoracic aorta was taken for follow-up experiments.

2.13. Hematoxylin-eosin staining

Mouse aortas were collected, fixed with conventional 4% paraformaldehyde, embedded in paraffin, and cut into 5 μm paraffin sections. The conventional HE dyeing operation was carried out. The paraffin sections were deparaffinized and rehydrated with gradient xylene and alcohol. Harris hematoxylin staining solution was used to stain the sections for 3–8 min, and the slices were washed with water. Eosin staining solution was used to stain the sections for 1–3 min. Gradient alcohol and xylene were used to dehydrate the slices. Then, the slices were dried and sealed with neutral gum and examined under a microscope, and images were collected and analyzed.

2.14. Immunohistochemistry staining

Immunohistochemistry experiments were used to stain the lipid components and transport-related proteins, including Abca1, Abcg1, Ldlr, Hdlbp, Lp-pla2, Srebp-1c, and Olr1, expressed in the aortic tissues of each group of mice. As before, conventional paraffin embedding and sectioning operations were performed. The sections were placed in a 10% BSA humidified box, sealed in a 37°C incubator, and incubated for 30 min. Antigen retrieval and blockade of endogenous peroxidase were carried out. Primary antibody dilutions (Olr1 (1:1000, DF6522, Affinity), Hdlbp (1:1000, ab133594, Abcam), Ldlr (1:100), Srebp-1c (1:100), Lp-pla2 (1:100), Abcg1 (1:100), Abca1 (1:100), and Gapdh (1:500)) were dropped onto the glass slides and incubated overnight. The next day, the slides were washed 3 times with PBS for 5 min each time. The secondary antibody (HRP-labeled) corresponding to the primary antibody was dropped onto the slice, the tissue was covered, and the slides were incubated at room temperature for 50 min. The freshly prepared DAB chromogenic solution was dripped onto the slices, and the color development time was controlled under a microscope. Hematoxylin was used to stain nuclei. After dyeing, neutral resin was used to seal the slices. The slides were examined using a microscope, and the images were collected and analyzed.

Table 2
The top 20 differentially expressed mRNAs (DEMs).

Gene symbol	$\log_2\text{FC}$	P value	t
LDLR	-3.060125	6.91E-12	21.88009
F13A1	-2.934125	1.09E-06	8.368071
MSMO1	-2.494237	1.13E-10	17.64917
MSMO1	-2.353523	2.17E-09	14.00167
SQLE	-2.349864	8.90E-12	21.46103
INSIG1	-2.120017	1.62E-10	17.15608
SQLE	-2.031948	1.83E-09	14.19146
FCGBP	-1.948243	6.51E-03	3.216984
CD93	-1.817352	7.00E-04	4.373945
ALOX5AP	-1.786447	6.28E-04	4.431864
DHCR7	-1.706983	2.91E-09	13.67849
GAPT	-1.691794	9.05E-06	6.909455
FADS1	-1.686854	1.22E-07	10.09117
VSIG4	-1.651483	4.92E-06	7.310877
IGF1	-1.603306	3.93E-04	4.684393
MS4A6A	-1.578847	1.45E-04	5.236591
HMGCS1	-1.54156	2.78E-08	11.40538
INSIG1	-1.527308	1.78E-06	8.01378
GIMAP7	-1.501859	2.42E-04	4.95066
HTR2B	-1.498137	4.47E-05	5.917596
Olr1	-1.461546	9.29E-06	6.892091

2.15. Statistical analysis

Experiments requiring statistical analysis were repeated three times. Experimental data are presented as the mean ± standard error. Statistical analysis was performed using SPSS software (version 13.0, SPSS, USA) with one-way ANOVA or two-way ANOVA followed by Tukey's test. A significant difference was declared if $P < 0.05$.

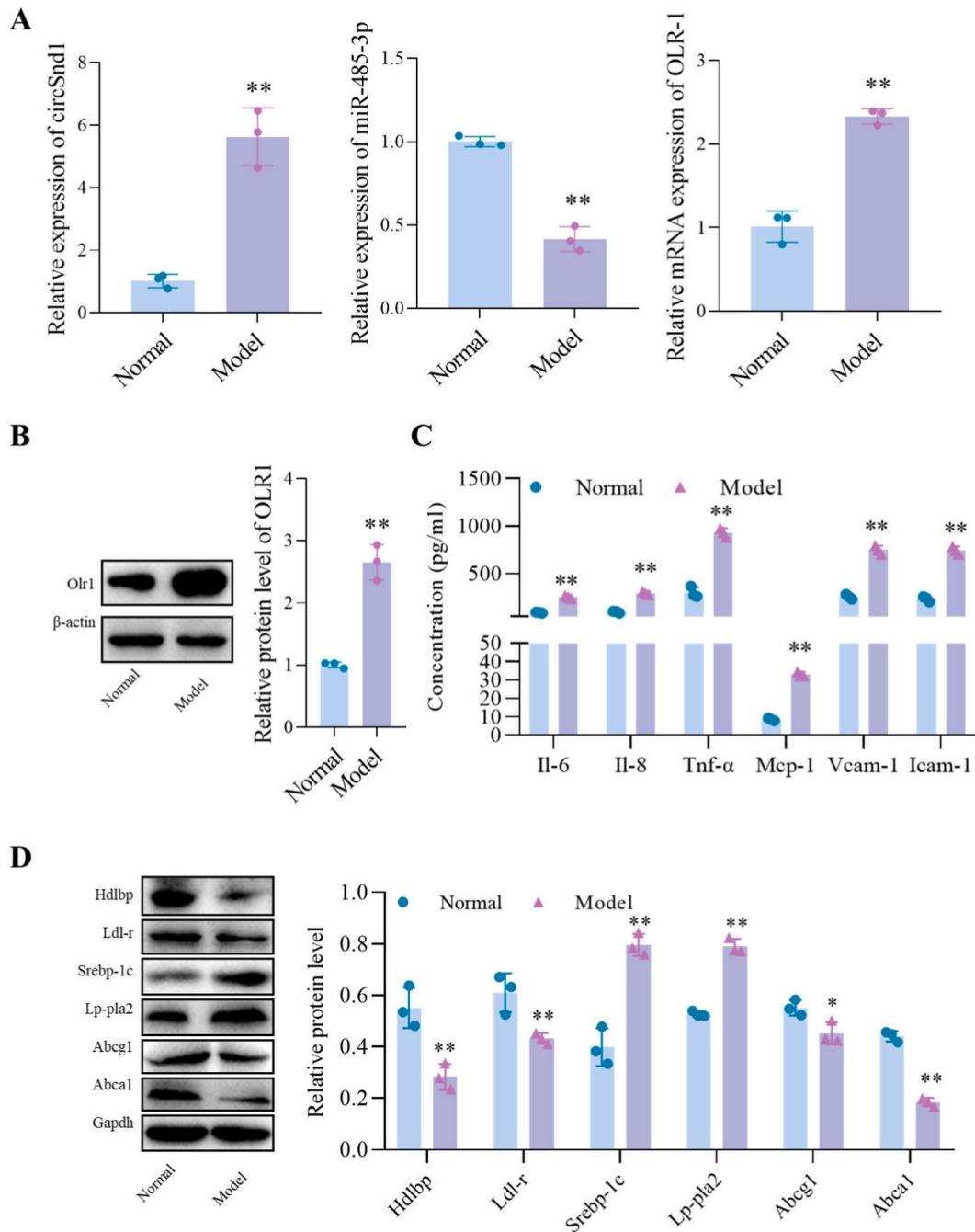


Fig. 2. Validation of the predicted genes in ox-LDL-induced mouse macrophages. A, circSnd1, miR-485-3p, and Olr1 mRNA expression verification. B, Olr1 protein expression verification. C, Verification of the expression changes in inflammatory signaling molecules possibly downstream of the circSnd1/miR-485-3p/Olr1 axis in mouse macrophages after treatment with ox-LDL. D, Changes in the expression of key proteins in lipid metabolism in ox-LDL-induced mouse macrophages. *, #p < 0.05; **, ##p < 0.01.

3. Results

3.1. circRNA-miRNA-mRNA ceRNA network

According to the cutoff criteria ($p < 0.05$ and $|\log_2FC| > 0.5$), a total of 29 differentially expressed circRNAs (DECs) and 497 differentially expressed mRNAs (DEMs) were identified between macrophages treated with and without ox-LDL in the GSE107522 and GSE54666 datasets, respectively (Fig. 1A). The IDs, sequences, and other detailed information of the 29 DECs are shown in Table 1, which contains 21 upregulated circRNAs and 8 downregulated circRNAs. The relevant information of the top 20 DEMs is shown in Table 2. A total of 497 DEMs were enriched in 25 pathways, mainly including ‘metabolic pathways’, ‘phagosome’, and ‘steroid biosynthesis’. Among them, the genes did not overlap across the above pathways, suggesting that these pathways in atherosclerosis may exert their function in their own ways. Due to the limited time and budget, we selected the ‘phagosome’ pathway, which is thought to be closely related to AS [18], after literature research. In this pathway, 18 genes were enriched, including 14 genes with low expression (*COLEC12*, *NCF1*, *NCF4*, *THBS2*, *CORO1A*, *TUBA1A*, *CLEC7A*, *CD209*, *HLA-DPB1*, *Olr1*, *CD14*, *FCGR2B*, *HLA-DOA*, and *HLA-DPA1*) and 4 genes with high expression (*DYNC1H1*, *CTSL*, *TUBB3*, and *CD36*) (Fig. 1B). The rest of the enriched pathways, such as ‘pathways in cancer’ and ‘osteoclast differentiation’, are seemingly not related to atherosclerosis. To further identify the specific genes that are closely related to AS, these 18 genes were subjected to subsequent construction and analysis of the ceRNA network. There were 377 predicted potential miRNAs targeting the 18 DEMs in the phagosome pathway and 208 predicted target miRNAs of the 29 DECs, which resulted in 136 intersecting miRNAs (Fig. 1C). Using Cytoscape, we showed the top 10 key nodes in the ceRNA

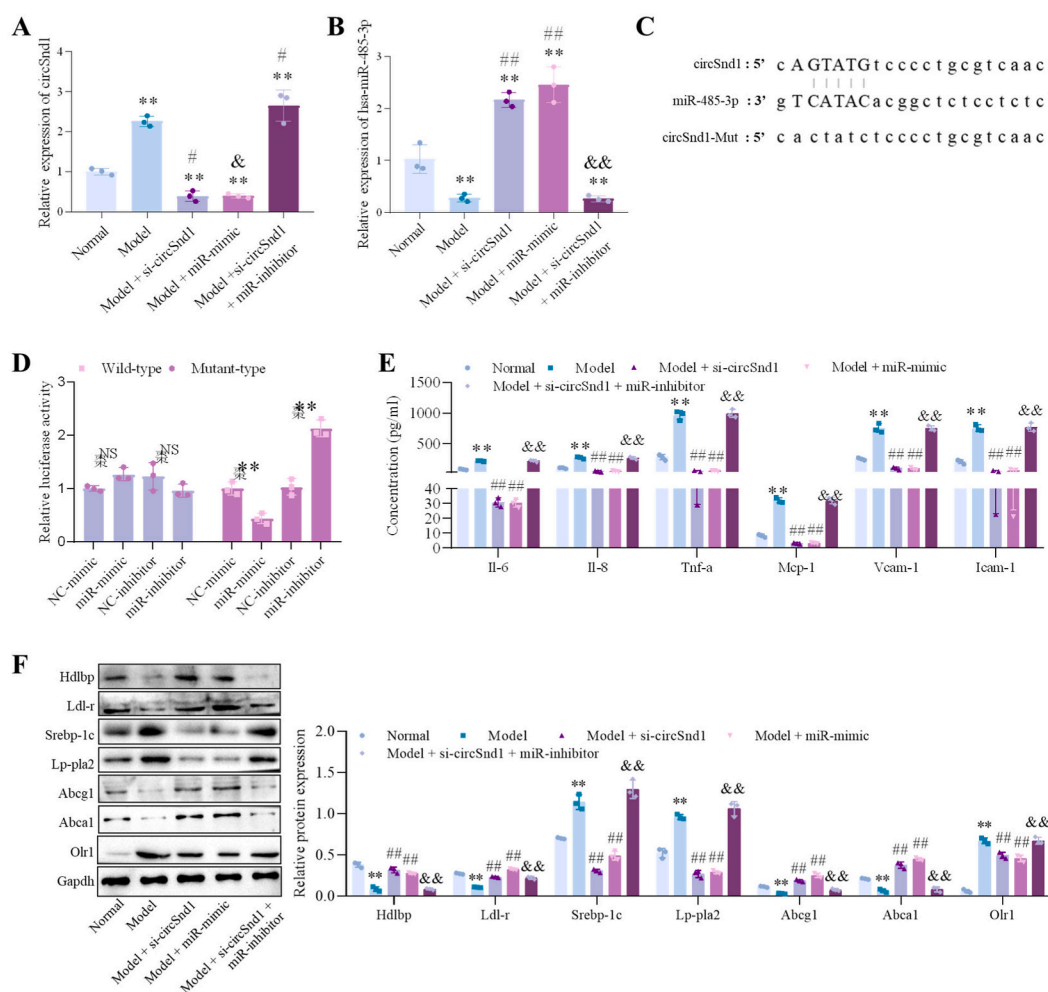


Fig. 3. circSnd1 targets miR-485-3p to regulate inflammation and lipid transport. A, The expression level of circSnd1 after manipulating the expression of circSnd1 and/or miR-485-3p in ox-LDL-induced macrophages using siRNA, miRNA mimic or inhibitor. B, The expression level of miR-485-3p after the alteration of circSnd1 and/or miR-485-3p in ox-LDL-induced macrophages. C-D, The binding sites of circSnd1 by miR-485-3p and its validation by the luciferase reporter experiment. E, Inflammatory factors were detected by ELISA. F, The protein expression of lipid composition and cholesterol transport indicators (Abca1, Abcg1, Ldlr, Hdlbp, Lp-pla2, and Srebp-1c) and Olr1. *, Compared with normal, # compared with model, & compared with si-circRNA. *, #, &, $p < 0.05$; **, ##, &&, $p < 0.01$.

network, including 5 circRNAs (hsa_circ_0007478, hsa_circ_0011279, hsa_circ_0082139 (namely, circSnd1), hsa_circ_0040921, and hsa_circ_0065149) and 5 mRNAs (*COLEC12*, *DYNC1H1*, *TUBA1A*, *Olr1*, and *THBS2*) (Fig. 1D–E). After further analysis of the core network, we found that *Olr1* might be in the core position, which is also supported by some related research. Of the 5 genes shown in Fig. 1D–E, *Olr1*'s function is well established in atherosclerosis, and *THBS2* has also been reported to play a role in arteriosclerosis [19]. Other genes, including *TUBA1A*, *DYNC1H1* and *COLEC12*, have yet to be reported to have clear associations with atherosclerosis. In addition, the role of the circRNA hsa_circ_0007478, which is associated with *THBS2* in this process, has also been reported in ox-LDL-treated macrophages [20]. Considering the research novelty and sequence conservation between mice and humans, we excluded *THBS2* and hsa_circ_0007478.

3.2. Dysregulated expression of circSnd1, miR-485-3p, and *Olr1* in an AS *in vitro* model

The levels of circSnd1, miR-485-3p, and *Olr1* mRNA were verified in mouse macrophages treated with ox-LDL. The results showed that circSnd1 and *Olr1* mRNA were highly expressed, and miR-485-3p expression was significantly lower after treatment with ox-LDL (Fig. 2A). These results were to some extent contrary to what we found in the public data (GSE107522 and GSE54666), where hsa_circ_0082139 and *Olr1* mRNA expression was lower in human macrophages after treatment with ox-LDL, although the positive correlation between hsa_circ_0082139 and *Olr1* mRNA was consistent. However, further western blotting results validated that *Olr1* was highly expressed at the protein level in the AS *in vitro* model (Fig. 2B and Figure S1). The experiments were repeated 3 times, and the results were consistent. In addition, the test results of inflammatory factors showed that the secretion levels of Il-6, Il-8, Tnf- α , Mcp-1, Vcam-1, and Icam-1 increased after ox-LDL treatment (Fig. 2C). The western blotting detection results of lipid transporters showed

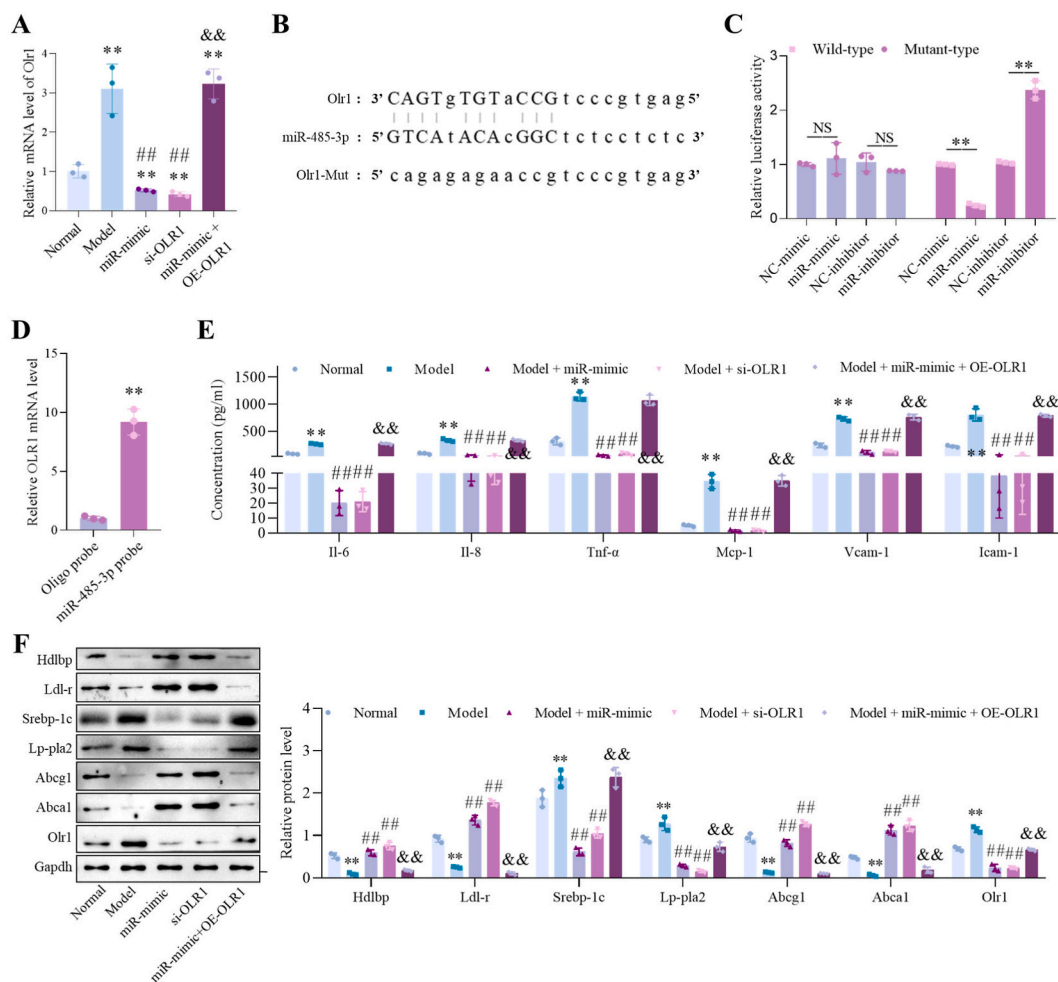


Fig. 4. miR-485-3p targets *Olr1* to regulate inflammation and lipid transport. A, *Olr1* mRNA expression in ox-LDL-induced mouse macrophages after altering the expression of miR-485-3p and/or *Olr1*. B–C, The binding site of miR-485-3p on the *Olr1* 3'-UTR and its verification through the luciferase reporter assay. D, The targeting relationship between miR-485-3p and *Olr1* was further proved using an RNA pull-down experiment. E, Inflammatory factors were detected by ELISA. F, The protein expression of lipid composition and cholesterol transport indicators and *Olr1*. *, Compared with normal, # compared with model, & compared with miR-mimic. *, #, &, $p < 0.05$; **, ##, &&, $p < 0.01$.

that the protein expression levels of Abca1, Abcg1, Ldlr, and Hdlbp were significantly reduced in the AS *in vitro* model, and the protein expression levels of Lp-pla2 and Srebp-1c were increased (Fig. 2D and Figure S2).

3.3. *circSnd1* interacts with *miR-485-3p* to regulate inflammation and lipid transport

The siRNA of *circSnd1* and mimics or inhibitor of *miR-485-3p* were transfected into macrophages individually or together to verify the targeting relationship between *circSnd1* and *miR-485-3p*. After interfering with *circSnd1*, the expression of *circSnd1* was

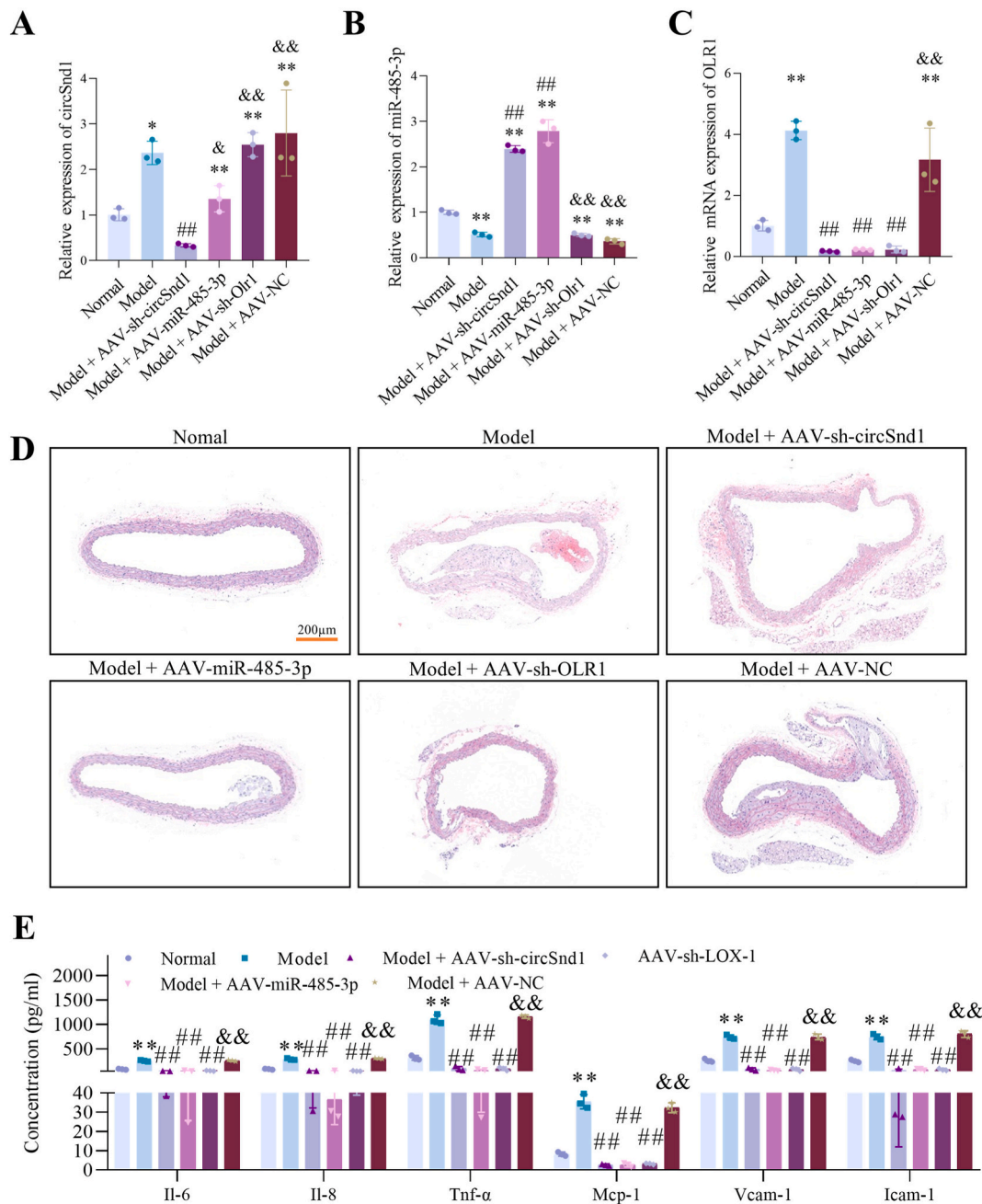
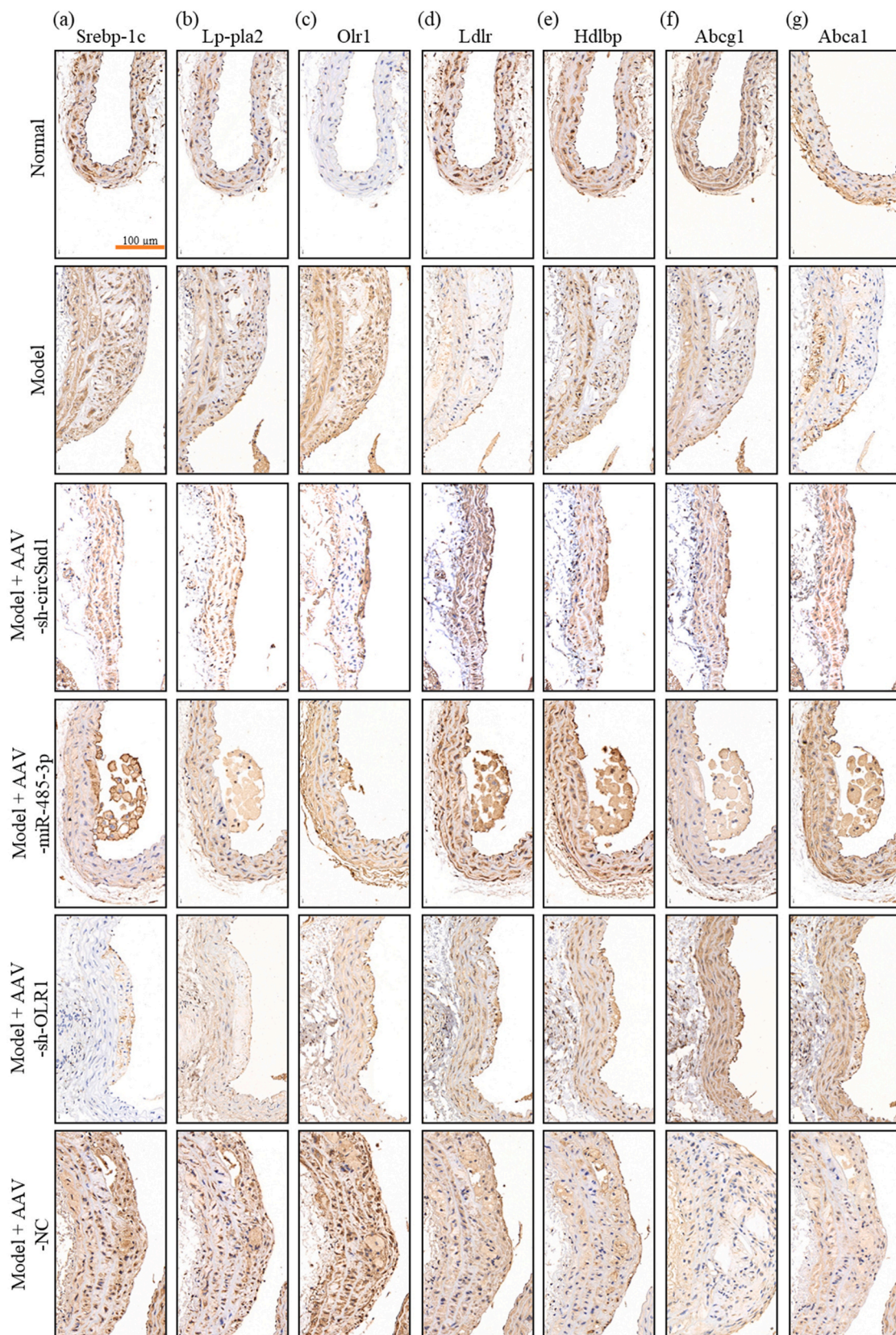


Fig. 5. *circSnd1*/*miR-485-3p*/*Olr1* affects the formation and development of AS by regulating inflammation and lipid transport in mice. A-C, The expression levels of *circSnd1* (A), *miR-485-3p* (B) and *Olr1* mRNA (C) after *circSnd1*, *miR-485-3p* and *Olr1* expression were altered in an atherosclerosis mouse model. D, Histomorphological changes in mouse aortas were detected by HE staining. Scale bar: 200 μm. E, Inflammatory factors were detected by ELISA. *, Compared with normal, # compared with model, & compared with sh-circRNA. *, #, &, p < 0.05; **, ##, &&, p < 0.01.



(caption on next page)

Fig. 6. Immunohistochemical staining for lipid composition and cholesterol transport indicators (Srebp-1c (a), Lp-pla2 (b), Olr1 (c), Ldlr (d), Hdlbp (e), Abcg1 (f), and Abca1 (g)) in the atherosclerotic lesions of aorta. Scale bar: 50 μ m.

confirmed to be knocked down, and miR-485-3p was found to be increased significantly compared to the model group; when the miR-485-3p inhibitor was cotransfected with si-circSnd1, the increase in miR-485-3p was blocked (Fig. 3A–B). The results of the luciferase reporter assay showed that the intensity of the luciferase vector containing wild-type circSnd1 was regulated by miR-485-3p (Fig. 3C–D). The fluorescence intensity decreased after miR-485-3p was overexpressed but increased after the miR-485-3p inhibitor was used. The fluorescence intensity of luciferase containing mutant circSnd1 was not regulated by the expression of miR-485-3p. The ELISA results showed that, compared to the model group, proinflammatory factors were significantly reduced after knocking down circSnd1 or overexpressing miR-485-3p, but the secretion of proinflammatory factors was reversed after knocking down circSnd1 and miR-485-3p at the same time (Fig. 3E). The western blotting results showed that after knocking down circSnd1 or overexpressing miR-485-3p, Olr1 and lipid composition and content indicators (Lp-pla2 and Srebp-1c) were expressed at low levels. However, after simultaneously knocking down circSnd1 and overexpressing miR-485-3p, this trend was restored (Fig. 3F and Figure S3). After knocking down circSnd1 or overexpressing miR-485-3p, the expression of the lipid transport-related proteins Abca1, Abcg1, Ldlr, and Hdlbp increased, while knocking down circSnd1 and overexpressing miR-485-3p resulted in restored levels (Fig. 3F and Figure S3).

3.4. miR-485-3p targets Olr1 to regulate lipid transport and is involved in AS formation

The miR-485-3p mimic and the overexpression plasmid or siRNA against Olr1 were separately transfected or cotransfected into macrophages to verify the targeting relationship between miR-485-3p and Olr1. After overexpression of miR-485-3p, the expression of Olr1 decreased, and after simultaneous overexpression of Olr1 and miR-485-3p, Olr1 expression was reversed (Fig. 4A). The luciferase reporter assay results showed that the fluorescence intensity of luciferase containing wild-type Olr1 gene fragments was regulated by the expression of miR-485-3p, while the fluorescence intensity of luciferase containing mutant Olr1 gene fragments was not affected by miR-485-3p expression (Fig. 4B–C). An RNA pull-down experiment was used to further prove the targeting relationship between miR-485-3p and Olr1 in cells. The results showed that the probe containing the miR-485-3p sequence had a significantly higher Olr1 mRNA content than the probe containing the negative control oligo sequence (Fig. 4D). The ELISA results showed that proinflammatory factors were significantly reduced compared to those in the model group after overexpression of miR-485-3p or knockdown of Olr1. However, after concurrent overexpression of miR-485-3p and Olr1, proinflammatory factors were increased (Fig. 4E). The western blotting results showed that after overexpression of miR-485-3p or knockdown of Olr1, lipid content indicators (Lp-pla2 and Srebp-1c) were expressed at low levels (Fig. 4F and Figure S4). After overexpressing miR-485-3p and Olr1 together, this trend was reversed. With overexpression of miR-485-3p or knockdown of Olr1, the expression of the lipid transport-related proteins Abca1, Abcg1, Ldlr, Hdlbp, and Olr1 increased, while overexpression of miR-485-3p with overexpression of Olr1 reversed this trend (Fig. 4F and Figure S4).

3.5. circSnd1/miR-485-3p/Olr1 affects the formation and development of AS by regulating inflammation and lipid transport in mice

The mouse AS model and AAV plasmids were used to further verify the effect of circSnd1/miR-485-3p/Olr1 on AS *in vivo*. AAV-sh-circSnd1, AAV-miR-485-3p and AAV-sh-Olr1 viruses were injected into mice. The PCR results showed that the expression level of circSnd1 was affected by AAV-sh-circSnd1 and AAV-miR-485-3p in the AS *in vivo* model (Fig. 5A). The expression level of miR-485-3p increased significantly after knocking down circSnd1 and overexpressing miR-485-3p (Fig. 5B). The expression of Olr1 mRNA decreased significantly after knocking down circSnd1, overexpressing miR-485-3p, and knocking down Olr1 in the AS model (Fig. 5C). The results of HE staining showed that, compared with the model group, knocking down circSnd1, overexpressing miR-485-3p, or knocking down Olr1 reduced the area of sclerosis in blood vessels to various degrees, but there was no significant change in the negative control group (Fig. 5D). The ELISA results showed that the expression levels of a variety of proinflammatory factors after knocking down circSnd1, overexpressing miR-485-3p, or knocking down Olr1 were significantly decreased, while the negative control group had no significant changes compared with the model group (Fig. 5E). The IHC results showed that, compared with the model group, knocking down circSnd1, overexpressing miR-485-3p, or knocking down Olr1 decreased the expression of the intravascular lipid content indices Lp-pla2 and Srebp-1c. Compared with the model group, knocking down circSnd1, overexpressing miR-485-3p, or knocking down Olr1 all increased the expression of lipid transport-related proteins, including Abca1, Abcg1, Ldlr, Hdlbp, and Olr1. As expected, there was no significant change in the negative control group, compared with the model group (Fig. 6a–g).

4. Discussion

In this study, we first obtained 29 circRNAs and 497 mRNAs of interest. Then, based on the literature and ceRNA network analysis, and accounting for time and budgetary limitations, we selected circSnd1/miR-485-3p/Olr1 for the following studies. Then, we validated the interaction of circSnd1 miR-485-3p and Olr1 mRNA in mouse macrophages after treatment with ox-LDL. Finally, we manipulated the expression of these genes both *in vitro* and *in vivo* using molecular tools, such as siRNA and AAV, and proved the potential function of this signaling axis in atherosclerosis. These findings may indicate that circRNA-mediated signals play at least a part in the formation and/or development of atherosclerosis.

In this study, the commonly used *APOE*^{-/-} or *LDLR*^{-/-} mice were not used to prepare the AS model, but a high-fat and high-cholesterol diet was used [1,21]. This is related to the relevant targets we selected. *APOE* and *LDLR* play key roles in lipid

metabolism processes, and the phagosome pathway and Olr1 we selected are mainly involved in lipid metabolism. BALB/c and C3H mice have comparable HDL levels, while C57BL/6 mice have much lower HDL levels, suggesting a tendency to develop atherosclerosis-like conditions [22]. Some researchers believe that the use of BALB/c mice on a cholate-containing diet for atherosclerosis research is a limitation, which will not be considered a standard model, as a cholate diet has additional proinflammatory effects. However, we have other opinions. Because the mechanism of atherosclerosis formation and development is multifaceted, we cannot exclude a model based only on inflammation status. To avoid the impact of APOE knockout on the experimental results and to obtain access to a feasible *in vivo* model, we chose C57BL/6 mice fed a high-fat and high-protein diet.

A large number of circRNAs are highly conserved and expressed in different types of cells. They have regulatory functions in human diseases and play a key role in the initiation and development of various types of biological processes [23]. The existing research mainly focuses on the sponge-absorbing role of miRNAs that indirectly regulates key molecules [24]. Research on the role of circRNAs in AS involves many aspects, for example, circRNA functions in endothelial cells and vascular smooth muscle cells as well as macrophages [5,7,25]. The sequence of the mature circSnd1 (for mouse, located on chr6: 28626099–28668658, circID: mmu_CIRCpedia_212934; for human, chr7: 127447537–127484477, circID: HSA_CIRCpedia_56501), whose host gene is Snd1, has 191 nucleotides and is conserved. Therefore, it can be studied in animals as a potential therapeutic target for atherosclerosis. Human circSnd1 has been shown to regulate the proliferation and migration of cancer cells, in which TNF- α may also be involved [26,27]. However, research on circSnd1 in atherosclerosis is not currently available. Here, through our experiments, we confirmed that knocking down circSnd1 can reduce the inflammation of macrophages by inhibiting Olr1 and reducing intracellular lipid accumulation and lipid transport.

As a direct target of circSnd1, miR-485-3p seemingly had a negative correlation with the development of atherosclerosis in our study. This finding is to some extent consistent with other reports. It was previously proven that in patients with coronary atherosclerosis, the level of exosomal miR-485-3p derived from epicardial adipose tissue was reduced, and in ox-LDL-treated RAW 264.7 cells, miR-485-3p was significantly decreased (according to GSE99685) [28,29]. However, a possibly contrary finding also exists. Plasmatic miR-485-3p was found to be increased in patients with coronary atherosclerosis disease [3]. However, these findings are probably not contradictory because this miRNA is not just from one type of cell (macrophages, VSMCs, and endothelial cells) or some specific tissue (plaque and blood vessel), even under the same conditions [30,31]. Therefore, the different roles of this miRNA in the cell types that matter in atherosclerosis may warrant further exploration.

Olr1 is a type II transmembrane glycoprotein with a size of 52 kD that belongs to the C-type lectin family. Olr1 is equivalent to CD36, SRA, and Toll-like receptors (TLRs) and is a scavenger receptor (SR) responsible for the binding, internalization, and degradation of ox-LDL [32]. By binding to these receptors, ox-LDL causes vascular endothelial cell damage and dysfunction and monocyte migration, induces cells to take up more ox-LDL, accelerates the transformation of macrophages into foam cells, and forms AS plaques under the vascular endothelium in the formation and development of AS [33], where mitogen-activated protein kinase, NF- κ B, NOX/ROS, and other pathways are closely involved [34]. Currently, Olr1 is considered to be a new target to alter the process of atherosclerosis, and reducing the expression of Olr1 is also considered a new strategy for AS treatment [35]. Here, we show that Olr1 participates in the process of AS by affecting inflammation and lipid transport, and this process can be regulated by circSnd1/miR-485-3p. Therefore, this study provides a new foundation for further clinical application of Olr1 as a treatment target.

Without question, the present study has some limitations and needs more in-depth studies. Firstly, circRNA is not broadly conserved among species like miRNA. When we confronted the screening of circRNAs and considered their further application in clinics, we actually didn't have much of choice, which may lead to the misunderstanding of some key regulatory mechanisms in human atherosclerosis that are quite different from those in animals. Secondly, the sample size in animal experiments is small, and therefore more animals are needed to further validate these findings. Thirdly, the study provides evidence of the potential therapeutic value of targeting this axis in AS treatment; however, clinical validation in human patients is needed to confirm these findings.

5. Conclusion

Overall, our results indicate that the regulation of Olr1 by circSnd1 and miR-485-3p in macrophage phagocytosis may have a significant impact on the formation and stability of atherosclerotic plaques. The circSnd1/miR-485-3p/Olr1 axis participates in the formation and progression of AS by influencing macrophage inflammation and lipid transport, in which circSnd1 acts as a ceRNA to sponge miR-485-3p and upregulate Olr1 expression. However, the main conclusion in this study may still require further evidence to support its use in clinical practice.

Ethics approval and consent to participate

This study was approved and supervised by the Animal Protection and Use Agency Committee of The First Affiliated Hospital of Xi'an Jiaotong University (approval number: 2019LSK-G-6).

Author contribution statement

Lin Yang: Conceived and designed the experiments; Performed the experiments, Analyzed and interpreted the data; Contributed reagents, materials, analysis tools or data; Wrote the paper.

Yuhao Lin and Chao Wang: Performed the experiments, Analyzed and interpreted the data; Contributed reagents, materials, analysis tools or data; Wrote the paper.

Pengcheng Fan: Performed the experiments, Analyzed and interpreted the data; Contributed reagents, materials, analysis tools or

data.

Data availability statement

Data will be made available on request.

Funding statement

This work was financially supported by the National Natural Science Foundation of China (No.: 81970365) and the Keyjoint Research and Invention Program of Shaanxi Province (No.: 2022SF-252).

Declaration of competing interest

The authors declare that they have no known competing financial interests or personal relationships that could have appeared to influence the work reported in this paper.

Acknowledgements

The language of this study was edited by American Journal Experts (AJE).

Appendix A. Supplementary data

Supplementary data related to this article can be found at <https://doi.org/10.1016/j.heliyon.2023.e17366>.

Figure S1. Original western blotting images of Fig. 2B; Olr1 (a) and β -actin (b).

Figure S2. Original western blotting images of Fig. 2D; Hdlbp (a), Ldl-r (b), Srebp-1c (c), Lp-pla2 (d), Abcg1 (e), Abca1 (f), and Gapdh (g).

Figure S3. Original western blotting images of Fig. 3F; Hdlbp (a), Ldl-r (b), Srebp-1c (c), Lp-pla2 (d), Abcg1 (e), Abca1 (f), Olr1 (g), and Gapdh (h).

Figure S4. Original western blotting images of Fig. 4F; Hdlbp (a), Ldl-r (b), Srebp-1c (c), Lp-pla2 (d), Abcg1 (e), Abca1 (f), Olr1 (g), and Gapdh (h).

References

- [1] B. Aryal, Y. Suárez, Non-coding RNA regulation of endothelial and macrophage functions during atherosclerosis, *Vasc. Pharmacol.* 114 (2019) 64–75.
- [2] D. Skuratovskaia, M. Vulf, A. Komar, E. Kirienkova, L. Litvinova, Promising directions in atherosclerosis treatment based on epigenetic regulation using microRNAs and long noncoding RNAs, *Biomolecules* 9 (2019) 226.
- [3] M.W. Feinberg, K.J. Moore, MicroRNA regulation of atherosclerosis, *Circ. Res.* 118 (2016) 703–720.
- [4] L. Yang, F. Yang, H. Zhao, M. Wang, Y. Zhang, Circular RNA circCHFR facilitates the proliferation and migration of vascular smooth muscle via miR-370/FOXO1/Cyclin D1 pathway, *Mol. Ther. Nucleic Acids* 16 (2019) 434–441.
- [5] J. Zhuang, T. Li, X. Hu, M. Ning, W. Gao, Y. Lang, W. Zheng, J. Wei, Circ_CHFR expedites cell growth, migration and inflammation in ox-LDL-treated human vascular smooth muscle cells via the miR-214-3p/Wnt3/beta-catenin pathway, *Eur. Rev. Med. Pharmacol. Sci.* 24 (2020) 3282–3292.
- [6] L. Wang, C. Shen, Y. Wang, T. Zou, H. Zhu, X. Lu, L. Li, B. Yang, J. Chen, S. Chen, Identification of circular RNA Hsa_circ_0001879 and Hsa_circ_0004104 as novel biomarkers for coronary artery disease, *Atherosclerosis* 286 (2019) 88–96.
- [7] H.-s. Huang, X.-y. Huang, H.-z. Yu, Y. Xue, P.-i. Zhu, Circular RNA circ-RELL1 regulates inflammatory response by miR-6873-3p/MyD88/NF- κ B axis in endothelial cells, *Biochem. Biophys. Res. Commun.* 525 (2020) 512–519.
- [8] W. Yang, W. Du, X. Li, A. Yee, B. Yang, Foxo3 activity promoted by non-coding effects of circular RNA and Foxo3 pseudogene in the inhibition of tumor growth and angiogenesis, *Oncogene* 35 (2016) 3919–3931.
- [9] A. Di Ruscio, A.K. Ebralidze, T. Benoukraf, G. Amabile, L.A. Goff, J. Terragni, M.E. Figueroa, L.L.D.F. Pontes, M. Alberich-Jorda, P. Zhang, DNMT1-interacting RNAs block gene-specific DNA methylation, *Nature* 503 (2013) 371–376.
- [10] L.M. Holdt, A. Stahringer, K. Sass, G. Pichler, N.A. Kulak, W. Wilfert, A. Kohlmaier, A. Herbst, B.H. Northoff, A. Nicolaou, Circular non-coding RNA ANRIL modulates ribosomal RNA maturation and atherosclerosis in humans, *Nat. Commun.* 7 (2016) 1–14.
- [11] J.-N. Boeckel, N. Jaé, A.W. Heumüller, W. Chen, R.A. Boon, K. Stellos, A.M. Zeiher, D. John, S. Uchida, S. Dimmeler, Identification and characterization of hypoxia-regulated endothelial circular RNA, *Circ. Res.* 117 (2015) 884–890.
- [12] A. Tajbakhsh, M. Rezaee, P.T. Kovanen, A. Sahebkar, Efferocytosis in atherosclerotic lesions: malfunctioning regulatory pathways and control mechanisms, *Pharmacol. Therapeut.* 188 (2018) 12–25.
- [13] L.S. Bisgaard, C.K. Mogensen, A. Rosendahl, H. Cucak, L.B. Nielsen, S.E. Rasmussen, T.X. Pedersen, Bone marrow-derived and peritoneal macrophages have different inflammatory response to oxLDL and M1/M2 marker expression—implications for atherosclerosis research, *Sci. Rep.* 6 (2016) 1–10.
- [14] J.-H. Li, S. Liu, H. Zhou, L.-H. Qu, J.-H. Yang, starBase v2.0: decoding miRNA-ceRNA, miRNA-ncRNA and protein–RNA interaction networks from large-scale CLIP-Seq data, *Nucleic Acids Res.* 42 (2014) D92–D97.
- [15] M. Kohl, S. Wiese, B. Warscheid, Cytoscape: software for visualization and analysis of biological networks, in: *Data Mining in Proteomics*, Springer, 2011, pp. 291–303.
- [16] W.W. Hauswirth, A.S. Lewin, S. Zolotukhin, N. Muzyczka, Production and purification of recombinant adeno-associated virus, *Methods Enzymol.* 316 (2000) 743–761, [https://doi.org/10.1016/s0076-6879\(00\)16760-6](https://doi.org/10.1016/s0076-6879(00)16760-6).
- [17] B. Paigen, P.A. Holmes, D. Mitchell, D. Albee, Comparison of atherosclerotic lesions and HDL-lipid levels in male, female, and testosterone-treated female mice from strains C57BL/6, BALB/c, and C3H, *Atherosclerosis* 64 (1987) 215–221.

- [18] R. Ganesan, K.M. Henkels, L.E. Wrenshall, Y. Kanaho, G. Di Paolo, M.A. Frohman, J. Gomez-Cambronero, Oxidized LDL phagocytosis during foam cell formation in atherosclerotic plaques relies on a PLD2-CD36 functional interdependence, *J. Leukoc. Biol.* 103 (2018) 867–883, <https://doi.org/10.1002/jlb.2a1017-407rr>.
- [19] S.M. Boekholdt, M.D. Trip, R.J. Peters, M. Engelen, J.M. Boer, E.J. Feskens, A.H. Zwinderman, J.J. Kastelein, P.H. Reitsma, Thrombospondin-2 polymorphism is associated with a reduced risk of premature myocardial infarction, *Arterioscler. Thromb. Vasc. Biol.* 22 (2002) e24–e27, <https://doi.org/10.1161/01.atv.0000046235.22451.66>.
- [20] B. Ye, X. Liang, Y. Zhao, X. Cai, Z. Wang, S. Lin, W. Wang, P. Shan, W. Huang, Z. Huang, Hsa_circ_0007478 aggravates NLRP3 inflammasome activation and lipid metabolism imbalance in ox-LDL-stimulated macrophage via miR-765/EFNA3 axis, *Chem. Biol. Interact.* 368 (2022), 110195, <https://doi.org/10.1016/j.cbi.2022.110195>.
- [21] L.F. Sun, D.Q. An, G.L. Niyazi, W.H. Ma, Z.W. Xu, Y. Xie, Effects of Tianxiangdan Granule treatment on atherosclerosis via NF- κ B and p38 MAPK signaling pathways, *Mol. Med. Rep.* 17 (2018) 1642–1650.
- [22] S. Oppi, T.F. Lüscher, S. Stein, Mouse models for atherosclerosis research—which is my line? *Front. Cardiovasc. Med.* 6 (2019) <https://doi.org/10.3389/fcvm.2019.00046>.
- [23] J. Salzman, Circular RNA expression: its potential regulation and function, *Trends Genet.* 32 (2016) 309–316.
- [24] X. Bao, S. Zheng, S. Mao, T. Gu, S. Liu, J. Sun, L. Zhang, A potential risk factor of essential hypertension in case-control study: circular RNA hsa_circ_0037911, *Biochem. Biophys. Res. Commun.* 498 (2018) 789–794.
- [25] L. Shen, Y. Hu, J. Lou, S. Yin, W. Wang, Y. Wang, Y. Xia, W. Wu, CircRNA-0044073 is upregulated in atherosclerosis and increases the proliferation and invasion of cells by targeting miR-107, *Mol. Med. Rep.* 19 (2019) 3923–3932.
- [26] L. Bai, W. Sun, Z. Han, H. Tang, CircSND1 regulated by TNF- α promotes the migration and invasion of cervical cancer cells, *Cancer Manag. Res.* 13 (2021) 259.
- [27] D. Wang, S. Zhang, D. Li, Q. Wang, Z. Xiao, Y. Zhang, CircSND1/miR-182-5p Axis promotes proliferative and invasive abilities of thyroid cancer via binding targeting MET, *J. Oncol.* 2022 (2022).
- [28] J. Liu, A. Gao, Y. Liu, Y. Sun, D. Zhang, X. Lin, C. Hu, Y. Zhu, Y. Du, H. Han, MicroRNA expression profiles of epicardial adipose tissue-derived exosomes in patients with coronary atherosclerosis, *Rev. Cardiovasc. Med.* 23 (2022) 206.
- [29] X. Li, S. Feng, Y. Luo, K. Long, Z. Lin, J. Ma, A. Jiang, L. Jin, Q. Tang, M. Li, Expression profiles of microRNAs in oxidized low-density lipoprotein-stimulated RAW 264.7 cells, *In Vitro Cell. Dev. Biol. Anim.* 54 (2018) 99–110.
- [30] C. Sangokoya, J.F. Doss, J.-T. Chi, Iron-responsive miR-485-3p regulates cellular iron homeostasis by targeting ferroportin, *PLoS Genet.* 9 (2013), e1003408.
- [31] J. Heo, H.C. Yang, W.J. Rhee, H. Kang, Vascular smooth muscle cell-derived exosomal microRNAs regulate endothelial cell migration under PDGF stimulation, *Cells* 9 (2020) 639.
- [32] T. Sawamura, N. Kume, T. Aoyama, H. Moriwaki, H. Hoshikawa, Y. Aiba, T. Tanaka, S. Miwa, Y. Katsura, T. Kita, T. Masaki, An endothelial receptor for oxidized low-density lipoprotein, *Nature* 386 (1997) 73–77, <https://doi.org/10.1038/386073a0>.
- [33] S. Tsimikas, E.S. Brilakis, E.R. Miller, J.P. McConnell, R.J. Lennon, K.S. Kornman, J.L. Witztum, P.B. Berger, Oxidized phospholipids, Lp (a) lipoprotein, and coronary artery disease, *N. Engl. J. Med.* 353 (2005) 46–57.
- [34] A.J. Kattoor, A. Goel, J.L. Mehta, LOX-1: regulation, signaling and its role in atherosclerosis, *Antioxidants* 8 (2019) 218.
- [35] N.V.K. Pothineni, S.K. Karathanasis, Z. Ding, A. Arulandu, K.I. Varughese, J.L. Mehta, LOX-1 in atherosclerosis and myocardial ischemia: biology, genetics, and modulation, *J. Am. Coll. Cardiol.* 69 (2017) 2759–2768.